HHS Public Access

Author manuscript

Chem Commun (Camb). Author manuscript; available in PMC 2016 August 18.

Published in final edited form as:

Chem Commun (Camb). 2015 August 18; 51(64): 12787–12790. doi:10.1039/c5cc03824c.

Nitroreductase-triggered activation of a novel caged fluorescent probe obtained from methylene blue

Jungeun Bae[a], **Louis E. McNamara**[b], **Manal A. Nael**[c], **Fakhri Mahdi**[d], **Robert J. Doerksen**[c], **Gene L. Bidwell III**[d], **Nathan I. Hammer**[b], and **Seongbong Jo**[a]

[a]Department of Pharmaceutics and Drug Delivery, School of Pharmacy, The University of Mississippi, University, MS 38677, USA

[b]Department of Chemistry and Biochemistry, The University of Mississippi, University, MS 38677, USA

[c]Department of BioMolecular Sciences, School of Pharmacy, The University of Mississippi, University, MS 38677, USA

[d]Department of Neurology, The University of Mississippi Medical Center, 2500 North State Street, Jackson, MS 39216, USA

Abstract

A near-infrared fluorescent probe based on methylene blue (*p*-NBMB) was developed for the detection of nitroreductase. Conjugating methylene blue with a *p*-nitrobenzyl moiety enables it to be activated by nitroreductase-catalyzed 1,6-elimination, resulting in the release of an active methylene blue fluorophore.

Graphical Abstract

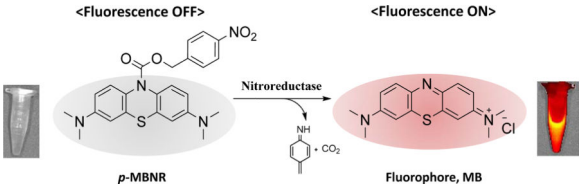

A new fluorescent probe caged with a p-nitrobenzyl redox switch enables selective switching on of fluorescence by nitroreductase.

Nitroreductase (NTR), a flavin mononucleotide (FMN) cofactor dependent protein expressed in *Escherichia coli* (*E. coli*), catalyzes reduction of a nitro group to hydroxylamine, which is subsequently converted to an amine in the presence of nicotinamide adenine dinucleotide phosphate (NAD(P)H) as a cofactor.[1] The large electronic change resulting from conversion of the electron-withdrawing nitro group to the electron-donating hydroxylamino group provides a selective ‘switch’ mechanism for the activation of an inert compound which leads to the subsequent release of the active agent. Based on this

Correspondence to: Seongbong Jo.

switch mechanism, various prodrug or activatable imaging probes have been designed with nitro groups as substrates to be triggered upon reduction by NTR.[2] The dicoumarin carbonate-based latent fluorophore was devised for the application in imaging to improve selectivity for NTR and aqueous solubility.[2b] Furthermore, NTR was employed in development of gene-directed enzyme prodrug cancer therapies (GDEPT), antibody-directed enzyme prodrug therapy (ADEPT) and drug screening as exemplified with 2,4-dinitrobenzamide (CB1954).[3] The basis of CB1954 activation has been fully elucidated and the molecule has advanced into clinical trials.[4]

Despite the previous extensive investigation about the use of nitrobenzyl redox switches for NTR activatable materials, these switches have not been applied for the development of bifunctional compounds, which can serve as a tool for selective imaging and therapy.[2–4] To design NTR activatable agents with combined imaging and therapeutic function, the selection of an appropriate reporter is of great importance. Among various reporters, fluorophores with emission in the far red and near-infrared (NIR), in the range of 600–1000 nm, are widely utilized in relevant research settings to overcome the limitation of poor tissue penetration owing to the interference from background auto-fluorescence from biomolecules.[5] In addition, NIR fluorophores offer several additional advantages over conventional imaging agents including high resolution, sensitivity and non-invasiveness.[6] In particular, methylene blue (MB) has been recognized as a sensible starting point for the development of a better NIR fluorophore given MB's strong absorption of broadband red light (550–700 nm, maximum at 664 nm), a wavelength at which absorption and autofluorescence are minimal.[7] Moreover, MB has been applied for clinical therapeutic purposes including treating methemoglobinemia, Barrett's esophagus, and cervical cancer.[8] MB is also known to be photodynamically active so that it can inactivate viruses, destroy bacteria, and inhibit cancer cell growth.[7b, 9] Given its advantageous properties, MB may be an ideal compound to use in design of an NTR-switchable probe with both imaging and therapeutic capability.

In this study, we describe a novel NIR fluorescent probe, *p*-nitrobenzyl 3,7-bis(dimethylamino)-10*H*-phenothiazine-10-carboxylate (*p*-NBMB) which can be triggered by NTR. To obtain a MB-based latent fluorescent probe, which is activatable, a *p*-nitrobenzyl moiety as an NTR switch was conjugated to cage MB at the nitrogen of the phenothiazine ring through a carbamate bond, thereby quenching electron transfer within the molecule (Scheme 1). This ultimately leads to improvements in achievable target-to-background auto-fluorescence ratios. In the presence of NTR, the resultant caged fluorescent probe is intended to be turned back on undergoing reduction of the aryl nitro group. Subsequently, the benzyl moiety will be removed by a rapid 1,6-elimination (Scheme 1). We primarily assessed the feasibility of whether a novel *p*-NBMB can be developed into an NTR selective activatable agent. Additionally, a potential therapeutic application of the compound in photodynamic therapy was also addressed.

The caged NIR fluorescent probe *p*-NBMB was synthesized in straightforward steps using MB and *p*-nitrobenzyl as shown in Scheme S1. Initially, MB in toluene (80% v/v in water) was reduced to obtain the activated leuco form of MB (leuco-MB). The yellow toluene phase containing leuco-MB was transferred into 4-nitrobenzyl chloroformate in toluene to

afford the caged *p*-NBMB. The orange solid resultant *p*-NBMB was characterized by elemental analysis and ^{1}H-NMR spectroscopy (ESI†). The proton NMR of *p*-NBMB in $CDCl_3$ in Fig. S1 showed all the characteristic peaks and splitting, which indicated successful *p*-NBMB synthesis. The chemical shift value of the two protons after the reaction was deshielded from 4.82 ppm to 5.32 ppm, which is indicative of the formation of the carbamate bond.

The spectral analysis of *p*-NBMB was compared with that of a fluorophore MB as a reference. In spectroscopic evaluation of MB and *p*-NBMB, MB exhibits maximal absorbance at 665 nm and fluorescence at 685 nm (λ_{ex} = 665 nm) (Fig. S2). In contrast, *p*-NBMB displayed neither significant absorbance nor fluorescence excitation at 665 nm. This phenomenon appears to be caused by the interruption of π-conjugation system bridging the three rings of MB, which quenches the absorbance between 500 nm to 800 nm. This result indicated that *p*-NBMB exhibits no fluorescence when the signal compound MB is caged with the nitrobenzyl moiety redox switch as illustrated in Scheme 1, which should lead to diminished noise in clinical imaging applications.

The selective uncaging via nitro reduction was assessed using NfsA, which is the major NTR from *E. coli*. As expected, *p*-NBMB exhibited a selective response for NTR, shown in Figure S3. The fluorescence spectrum of the control revealed no emission between 640 and 800 nm when excited by either 580 nm light using a fluorescence spectrometer or by 514.5 nm laser light, unless NTR is added in the solution. Heterogeneities of reduced *p*-NBMB were further observed with thin film fluorescence emission spectra as shown in Fig. 1. After reduction of *p*-NBMB by NTR, several different peaks were recovered in addition to the dominant 680 nm peak in the spectrum (Fig. 1). These results might be due to the formation of aggregates and excimers when the reduced *p*-NBMB interacts with the surface of a glass cover slip. A previous reported study also showed that the fluorophore MB forms dimers in dilute aqueous solutions and aggregates at increasing concentration due to the strong π-interactions among MB molecules.[10] Thus, peaks from dimer and aggregates would appear on the longer wavelength at 712 nm and 728 nm due to the transition dipole moment from the ground state to the lower excited state, called the N-branch.[11] Considering the increase in fluorescence intensity in the presence of NTR, we anticipate that uncaging *p*-NBMB is dependent on nitroreductase-mediated two-electron reduction of the nitrobenzyl moiety redox switch.

To verify whether there is a fluorescence response to other redox enzymes, which catalyze two-electron reduction, *p*-NBMB emission was investigated using DT-diaphorase. As shown in Fig. S4, DT-diaphorase did not induce any noticeable fluorescence signal enhancement from *p*-NBMB compared to the negative control without the enzyme, over an incubation period up to 48 h. According to previous studies on triggerable fluorescent probes, nitrobenzimidazoles containing aryl nitro groups could be an efficient redox switch that can be turned on by DT-diaphorase.[12] In addition, CB1954, the aforementioned prodrug carrying aryl nitro groups, was found to be activated by both DT-diaphorase and NTR but NTR

†Electronic Supplementary Information (ESI) available: [details of any supplementary information available should be included here]. See DOI: 10.1039/x0xx00000x

catalyzed the reduction of CB1954 60 times faster than DT-diaphorase.[4, 13] However, caged *p*-NBMB with the *p*-nitrobenzyl modification on the phenothiazine ring was not activated by DT-diaphorase. The result indicated that *p*-NBMB can be selectively reduced in the presence of NTR and hence can be used for NTR detection.

We also examined changes in fluorescence intensity as a function of concentration of *p*-NBMB, following incubation with one unit/ml of NTR. An increase in fluorescence intensity was observed when the concentration of *p*-NBMB was increased from 1 to 10 to 100 μM (Fig. 2). This result indicates that fluorescence enhancement is dependent on reduction of a *p*-nitrobenzyl redox switch by NTR. However, based on qualitative interpretation, the fluorescence intensity was not proportional to the concentration of *p*-NBMB within the concentration range. From this result, we inferred that the fluorescence enhancement would be more related to the amount of NTR. Hence, two concentrations of NTR, 1 unit/mL and 2 units/mL, were tested to observe the redox enzyme capacity in releasing fluorophore MB from *p*-NBMB (Fig. S5, ESI†). At the lowest *p*-NBMB concentration, 1 μM, the higher fluorescence emission intensity was similar, regardless of NTR concentrations. This implies that *p*-NBMB might show a detection limit at *p*-NBMB concentrations higher than 1 μM. For better visualization, we investigated the imaging capacity of *p*-NBMB using an *in vivo* imaging system, a Xenogen IVIS® Spectrum. As expected from the result showing NTR dependent fluorescence release in Fig. 3, images obtained from IVIS® are consistent. When the fluorescence intensity was compared by the released radiance efficiency *in vivo*, there were no statistically significant differences between the two *p*-NBMB concentrations. These results suggest that fluorescence emission occurring by *p*-NBMB reduction was predominantly dependent on the reduction capacity of NTR in the presence of NAD(P)H, providing its potential use for monitoring NTR.

Since we are interested in *p*-NBMB application not only in NTR activatable imaging *in vitro* but also for therapeutic purposes, we primarily focused on the characterization of the NTR selectivity of *p*-NBMB. This can be eventually translated into therapeutic advances in photodynamic therapy using fluorophores. Hence, we further examined the fluorescence response of *p*-NBMB to intact *E. coli* K12 strain XL1-Blue. When incubated with 10^9 CFU/mL of *E. coli,* the NIR fluorescent probe *p*-NBMB was activated and released a fluorophore showing emission as indicated in the images in Fig. 4. In addition, *p*-NBMB demonstrated a concentration dependent increase in fluorescence intensity in the presence of bacteria. When the *p*-NBMB concentration is 1 μM as this bacterial concentration, no noticeable change in fluorescence emission was observed, indicating that the detection limit is 1 μM. This result is consistent with Fig. S5. We also used a serial dilution of a bacterial suspension to determine *in vitro* sensitivity of *p*-NBMB fluorescence to bacterial number (see ESI†). As shown in Fig. S6, the raw fluorescence images and the quantified data indicated that fluorescence intensity from *p*-NBMB is correlated with an increase in bacterial number. At the concentration and incubation time shown, the detection limit ranged between 10^7 and 10^8 CFU/mL. However, optimizing concentration of *p*-NBMB and incubation time could likely increase this limit. These observations implied that *E. coli* expressing NTR activates reduction of a redox switch in *p*-NBMB to facilitate release of a fluorophore, MB.

Along with the capacity of *p*-NBMB for imaging anaerobic bacteria expressing NTR, *p*-NBMB might be useful for the detection of hypoxia in application for tumor diagnosis based on the recently reported studies demonstrating that molecular probes caged with nitrobenzyl group showed fluorescence enhancement in hypoxia condition (1% pO_2).[15] Moreover, since the fluorophore methylene blue is an effective photosensitizer for photodynamic therapy, the generation of singlet oxygen ($^1O_2$) from *p*-NBMB was tested using *p*-nitrosodimethylaniline (RNO) before and after activation by NTR. It is known that RNO is bleached in the presence of single oxygen, implying that the change in RNO absorbance intensity indicates the generation of $^1O_2$.[16] Figure S7a shows that the *p*-NBMB incubated with NTR/NAD(P)H exhibited a decrease in RNO absorbance after laser irradiation at a wavelength of 634 nm (110 mW/cm^2, Hughes Research Laboratories, Culver City, CA). In contrast, no significant change in RNO absorbance was observed from the control after laser exposure (Fig. S7b). This result indicated that free MB released from *p*-NBMB reduction was able to generate $^1O_2$ upon an irradiation in a NIR range. Based on the work done by Komine *et al.* demonstrating that $^1O_2$ generated from MB (0.01%) with a laser irradiation for 5 min killed *E. faecalis* (>99.9%)[17], *p*-NBMB will be beneficial both for targeted diagnostic and therapeutic applications.

Molecular docking was also exploited to predict the accessability of the active site of NTR to *p*-NBMB.[18] The docking results revealed that the ten generated poses of *p*-NBMB fit well inside the binding pocket of NTR based on FRED Chemgauss 4 scores in the range of −11 to −9 (Fig. 5). By inspecting the binding mode of *p*-NBMB, shown in Fig. S8, we noticed that one phenyl ring of the phenothiazine skeleton forms a π-π stacking interaction with Arg15, the positively charged amino group interacts with the negatively charged carboxylate of Glu162, and the carbamate carbonyl forms a dipole cation interaction with Lys167 (Fig. S8). These results rationally correlate favorable *p*-NBMB binding to the active site of NTR and the experimental observation of efficient *p*-NBMB reduction by NTR.

We have developed a new NIR fluorescent probe *p*-NBMB equipped with a *p*-nitrobenzyl redox switch that enables selective switching on of fluorescence by NTR. Whereas *p*-NBMB shows no fluorescence emission in PBS buffer at pH 7.4, it exhibits remarkable NIR fluorescence intensity after undergoing selective reduction by NTR. Furthermore, *p*-NBMB fluorescence was induced by incubation with live *E. coli* bacteria, indicating that endogenous NTR can activate the nitrobenzyl moiety switch to generate the fluorophore. This collectively indicates that *p*-NBMB would be a suitable imaging sensor to detect bacteria expressing NTR. In addition, *p*-NBMB also possesses potential as an MB prodrug which can be applied for the treatment of various diseases.

Supplementary Material

Refer to Web version on PubMed Central for supplementary material.

Acknowledgments

We acknowledge that funding for this work from the Department of Defense W81XWH-10-1-0414 (S.J.). This work was also supported in part by NSF funding from CHE-0955550 (N.I.H.)

Partial funding for this work came from EPS-1006883 (R.J.D.). This work is partially supported by National Science Foundation EPS-0903787 (S.J., N.I.H., and R.J.D.) This work was also conducted in part in a facility constructed with support from Research Facilities Improvements Program (C06 RR-14503-01) from the NIH National Center for Research Resources. The Animal Imaging Core Facility at the University of Mississippi Medical Center Cancer Institute performed imaging for this study.

Notes and references

1. Palmer BD, van Zijl P, Denny WA, Wilson WR. J. Med. Chem. 1995; 38:1229–1241. [PubMed: 7707325]
2. (a) Searle PF, Chen MJ, Hu L, Race PR, Lovering AL, Grove JI, Guise C, Jaberipour M, James ND, Mautner V. Clin. Exp. Pharmacol. Physiol. 2004; 31:811–816. [PubMed: 15566399] (b) Huang H-C, Wang K-L, Huang S-T, Lin H-Y, Lin C-M. Biosens. Bioelectron. 2011; 26:3511–3516. [PubMed: 21398106]
3. Denny WA. Curr. Pharm. Des. 2002; 8:1349–1361. [PubMed: 12052212]
4. Knox RJ, Friedlos F, Sherwood RF, Melton RG, Anlezark GM. Biochem. Pharm. 1992; 44:2297–2301. [PubMed: 1472095]
5. (a) Schaeffter, T. Imaging in Drug Discovery and Early Clinical Trials. Vol. 62. Birkhäuser Basel: 2005. ch. 2; p. 15-81.(b) Filonov GS, Piatkevich KD, Ting LM, Zhang J, Kim K, Verkhusha VV. Nat. Biotechnol. 2011; 29:757–761. [PubMed: 21765402]
6. (a) Benaron D. Cancer Metastasis Rev. 2002; 21:45–78. [PubMed: 12400996] (b) Willmann JK, van Bruggen N, Dinkelborg LM, Gambhir SS. Nat. Rev. Drug Discov. 2008; 7:591–607. [PubMed: 18591980]
7. (a) Tanaka E, Chen FY, Flaumenhaft R, Graham GJ, Laurence RG, Frangioni JV. J. Thorac. Cardiovasc. Surg. 2009; 138:133–140. [PubMed: 19577070] (b) Tang W, Xu H, Kopelman R, Philbert MA. Photochem. Photobiol. 2005; 81:242–249. [PubMed: 15595888]
8. (a) Wendel WB. J. Clin. Investigation. 1939; 18:179.(b) Ormeci N, Savas B, Coban S, Palabıyıkoğlu M, Ensari A, Kuzu I, Kursun N. Surg. Endosc. 2008; 22:693–700. [PubMed: 17704887]
9. (a) Wagner M, Suarez E, Theodoro T, Machado Filho C, Gama M, Tardivo J, Paschoal F, Pinhal M. Clin. Exp. Derma. 2012; 37:527–533.(b) Floyd RA, Schneider JE, Dittmer DP. Antiviral Res. 2004; 61:141–151. [PubMed: 15168794] (c) Perdrau J, Todd C. Proc. R. Soc. Lond. B Biol. Sci. 1933:288–298.(d) Tardivo JP, Del Giglio A, de Oliveira CS, Gabrielli DS, Junqueira HC, Tada DB, Severino D, de Fátima Turchiello R, Baptista MS. Photodiagnosis Photodyn. Ther. 2005; 2:175–191. [PubMed: 25048768]
10. (a) Fornili SL. J. Chem. Soc. Faraday Trans. 1981; 77:3049.(b) Heger D. J. Phys. Chem. A. 2005; 109:6702–6709. [PubMed: 16834023] (c) Jockusch S, Turro NJ, Tomalia DA. Macromolecules. 1995; 28:7416–7418.
11. Patil K, Pawar R, Talap P. Phys. Chem. Chem. Phys. 2000; 2:4313–4317.
12. Anusevičius Ž, Nivinskas H, Segura-Aguilar J. Arch. of Biochem. Biophys. 1997; 346:219–229. [PubMed: 9343369]
13. Anlezark GM, Melton RG, Sherwood RF, Coles B, Friedlos F, Knox RJ. Biochem. Pharm. 1992; 44:2289–2295. [PubMed: 1472094]
14. Schrödinger Release 2015-1: Maestro, version 10.1. New York, NY: Schrödinger, LLC; 2015.
15. Guo T, Cui L, Shen J, Zhu W, Xu Y, Qian X. Chem. Commun. 2013; 49:10820–10822.
16. Kraljic I, Mohsni SE, Arvis M. Photochem. Photobiol. 1978; 27:531–537.
17. Komine C, Tsujimoto Y. J. Endodont. 2013; 39:411–414.
18. McGann M. J. Chem. Info. Model. 2011; 51:578–596.

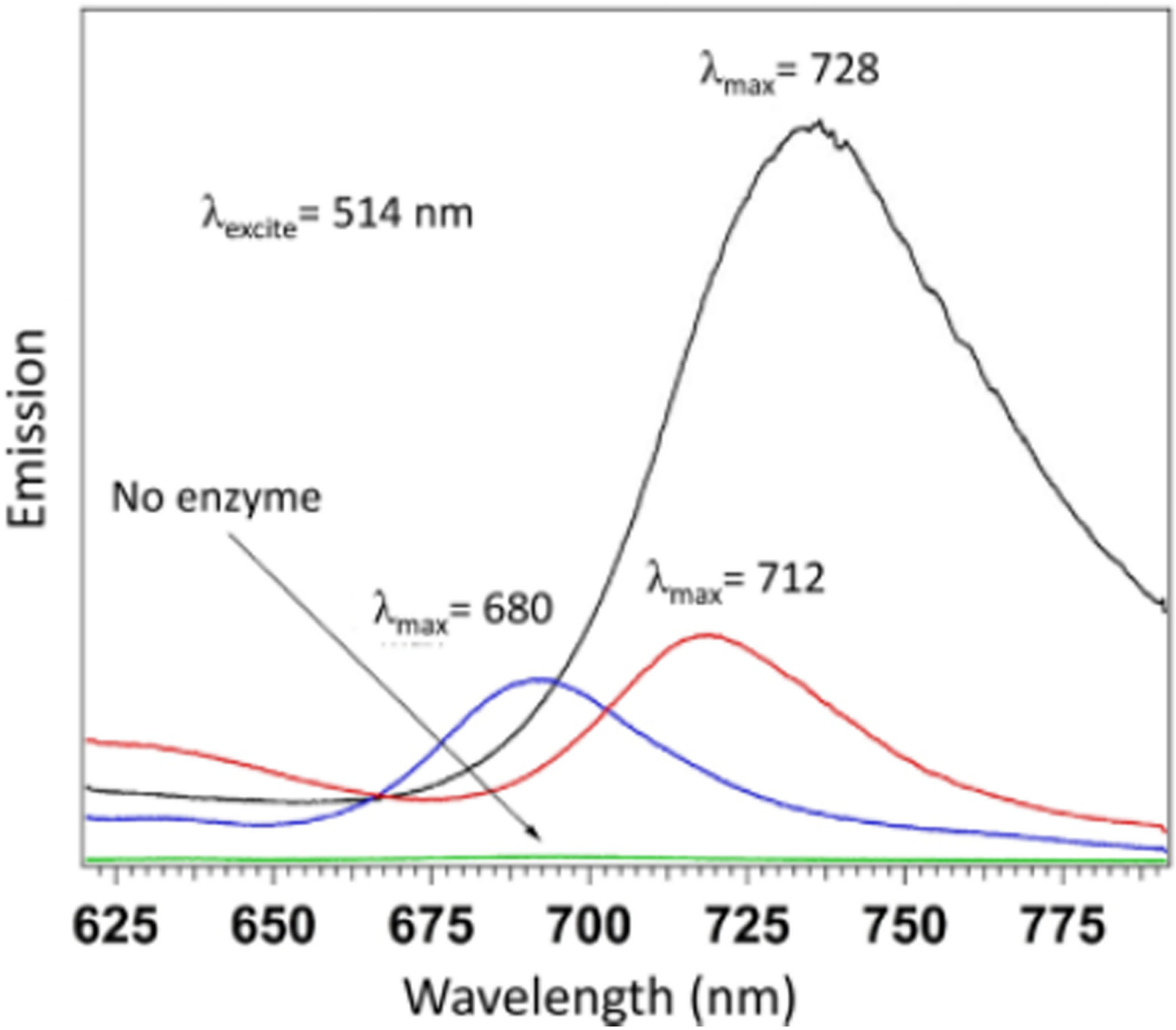

Fig. 1.

Heterogeneity of *p*-NBMB in addition of NTR (1 unit) with NAD(P)H (1 mM). Thin film fluorescence emission spectra were obtained at 541 nm excitation.

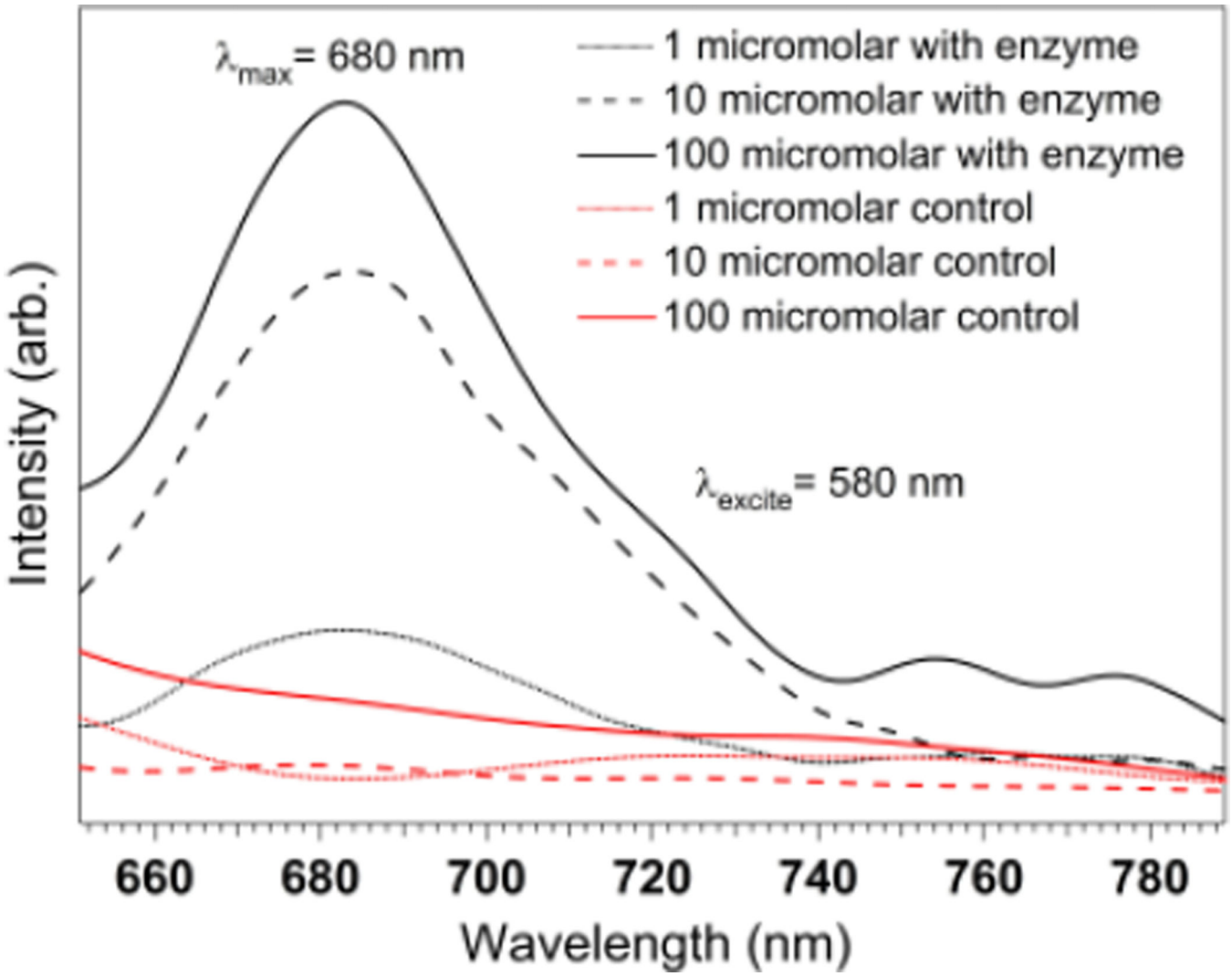

Fig. 2.

Fluorescence spectra of *p*-NBMB (1 μM, 10 μM, 100 μM) with NTR (1 unit) in the presence of NAD(P)H (1 mM) and the negative control without NTR. Spectra were acquired in 10 mM PBS, pH 7.4 with the excitation at 580 nm.

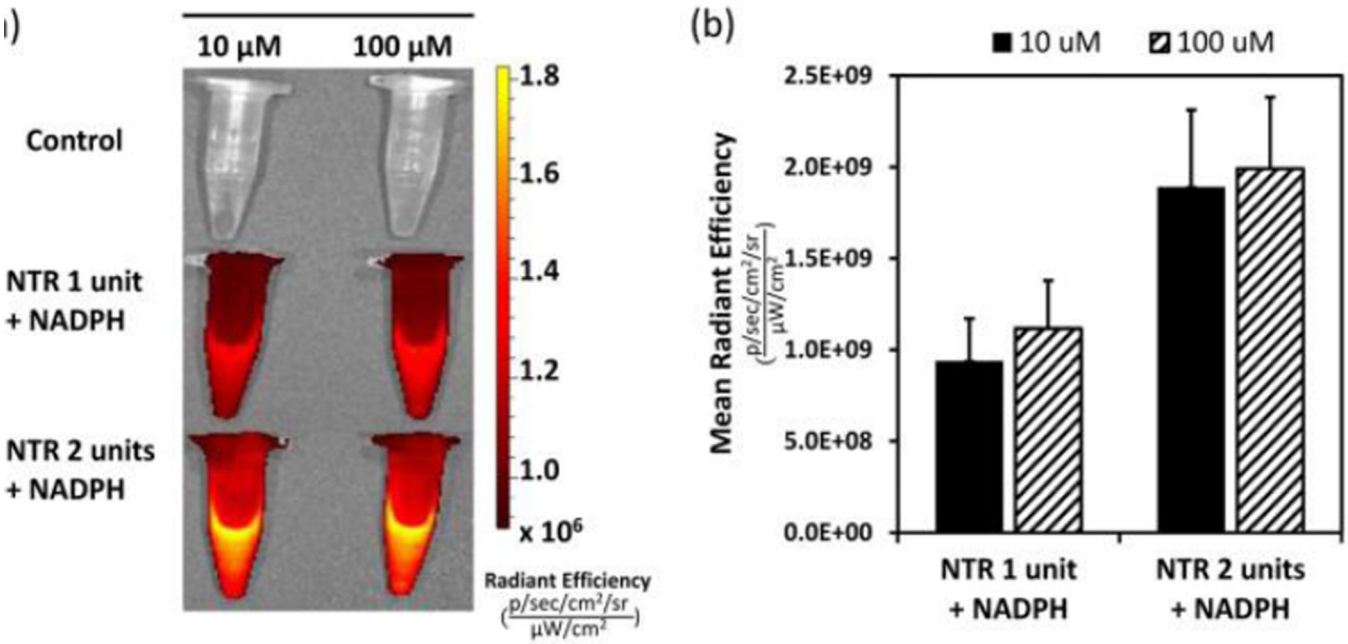

Fig. 3.

Fluorescence response of p-NBMB to nitroreductase. (a) IVIS fluorescence images of *p*-NBMB (10 µM, 100 µM) with nitroreductase (1 and 2 unit/ml, 1 mM NAD(P)H) and the control without nitroreductase. (b) Quantitation of fluorescence from each group. Data shown as mean ± SD (n = 3). Spectra were acquired after incubation at 37 °C overnight in 10 mM PBS (pH 7.4).

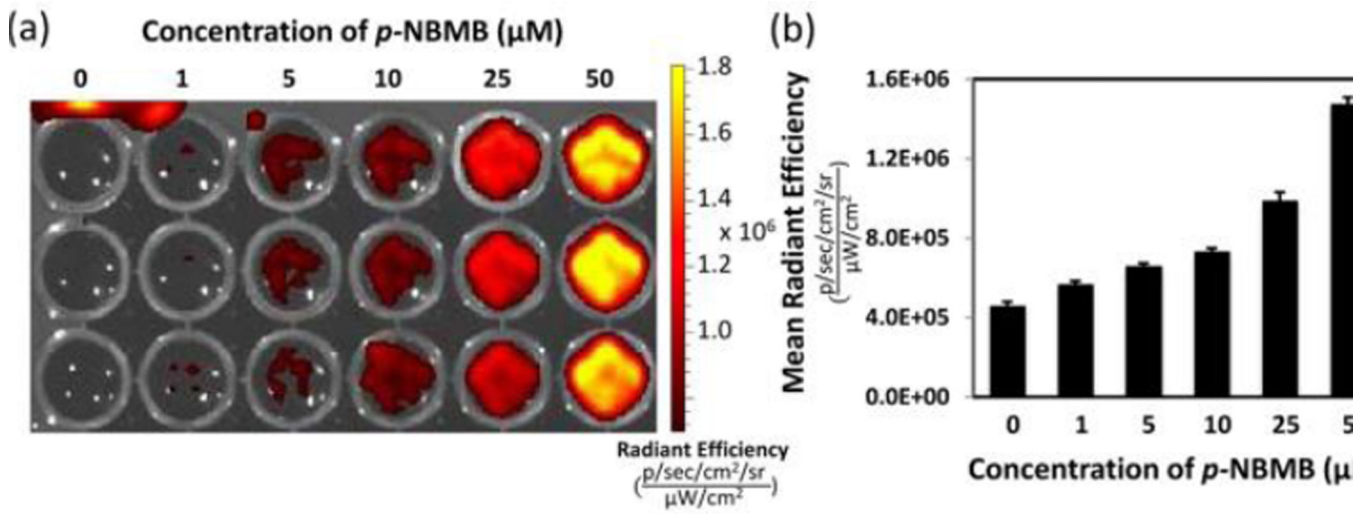

Fig. 4.

IVIS fluorescence images of *p*-NBMB (1 – 50 μM) incubated with intact *E. coli* K12 strain XL1-Blue (10^9 CFU/mL) at 37 °C for 4 hours.

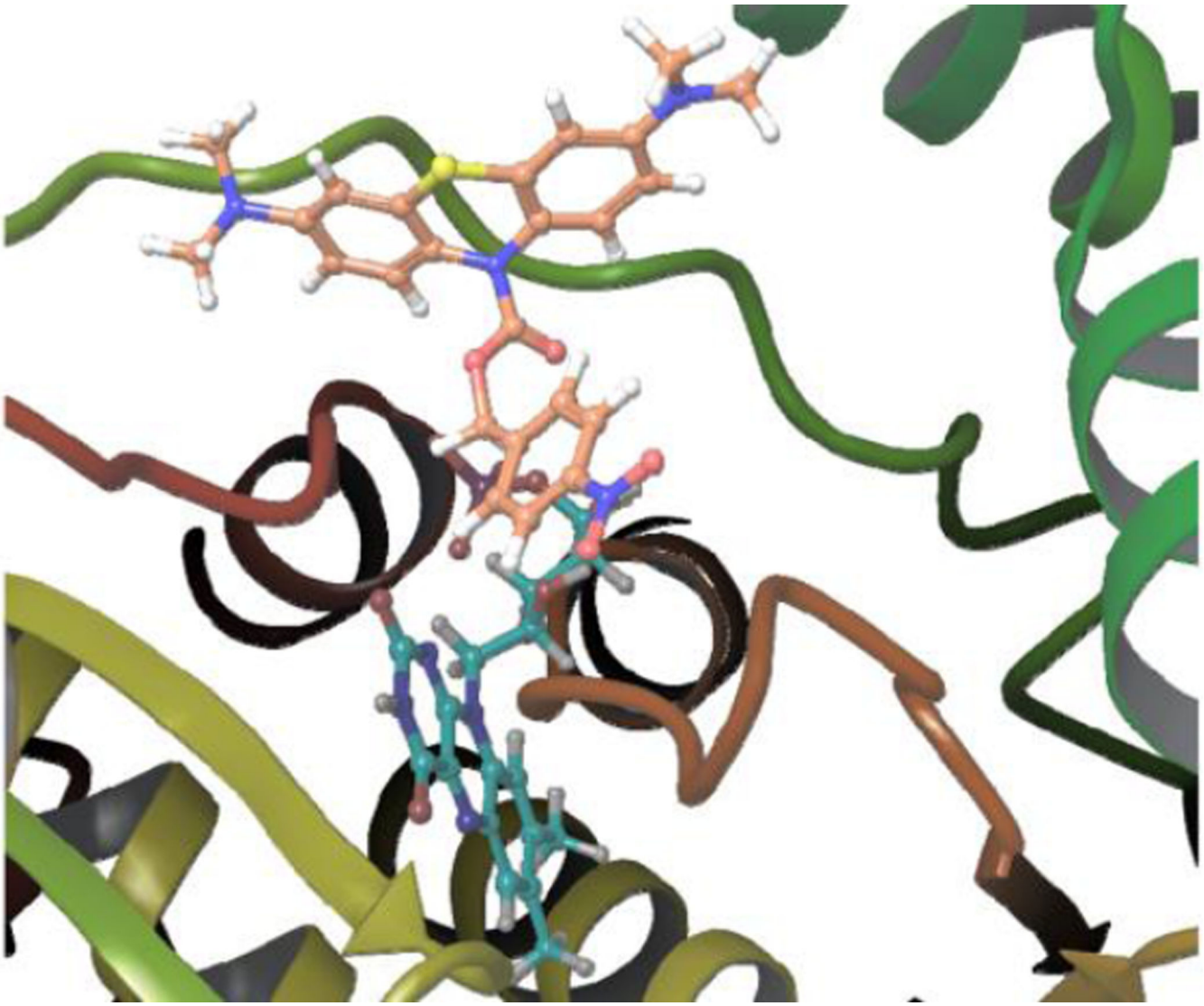

Fig. 5.

The best binding pose of *p*-NBMB (orange carbons) to NTR. FMN is shown as cyan carbons. The substrate binding pocket of NTR (PDB 1F5V) was generated using Fred v3.0.0 of OpenEye software suite. The enzyme is represented as cartoon and colored by secondary structure (prepared with Maestro[14]).

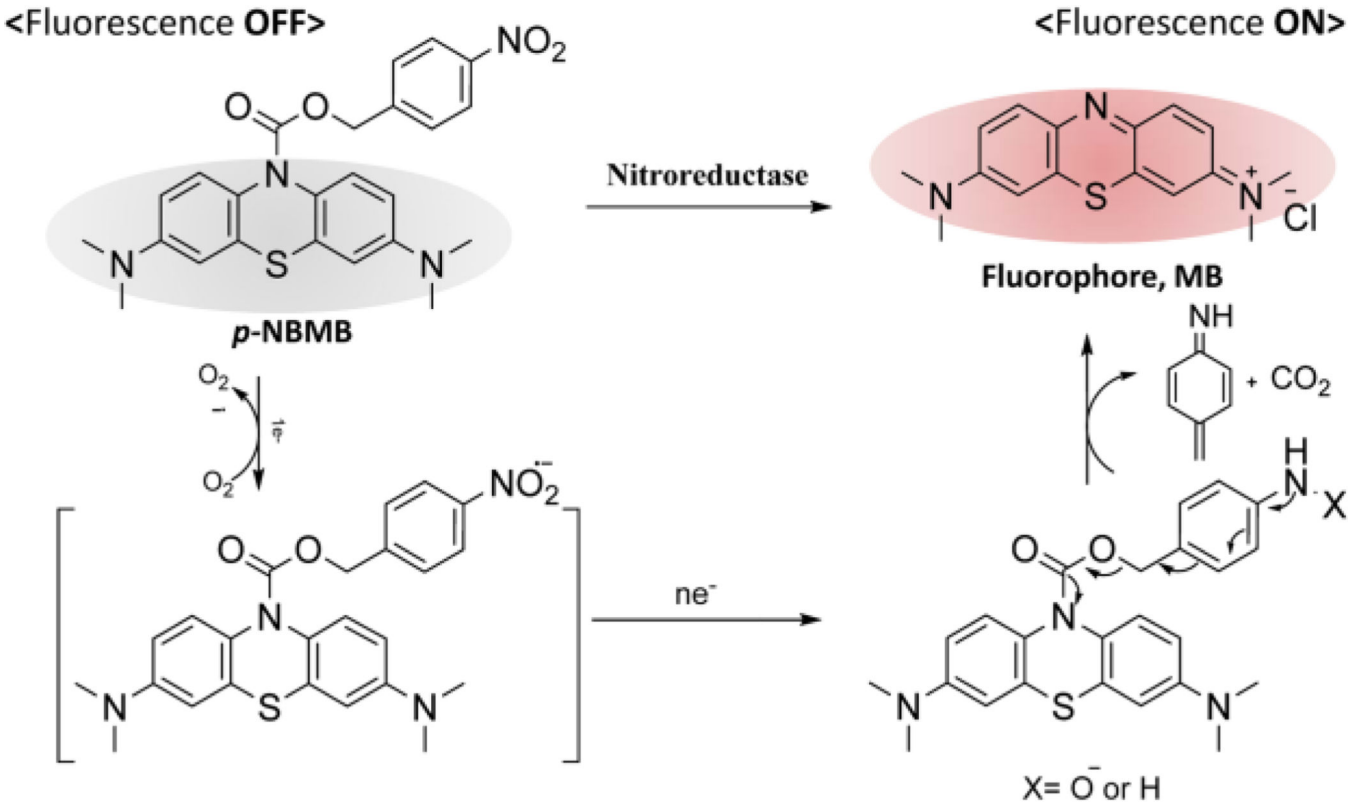

Scheme 1.

Mechanism of switching on the fluorescence probe, *p*-NBMB, upon reduction of a *p*-nitrobenzyl moiety after nitroreductase-mediated activation.